



Enhanced graph-based fault diagnostic system for nuclear power plants

Yong-Kuo Liu^{1,2} · Xin Ai² · Abiodun Ayodeji² · Mao-Pu Wu³ · Min-Jun Peng² · Hong Xia² · Wei-Feng Yu²

Received: 27 June 2019/Revised: 15 August 2019/Accepted: 20 August 2019/Published online: 14 November 2019
© China Science Publishing & Media Ltd. (Science Press), Shanghai Institute of Applied Physics, the Chinese Academy of Sciences, Chinese Nuclear Society and Springer Nature Singapore Pte Ltd. 2019

Abstract Scheduled maintenance and condition-based online monitoring are among the focal points of recent research to enhance nuclear plant safety. One of the most effective ways to monitor plant conditions is by implementing a full-scope, plant-wide fault diagnostic system. However, most of the proposed diagnostic techniques are perceived as unreliable by operators because they lack an explanation module, their implementation is complex, and their decision/inference path is unclear. Graphical formalism has been considered for fault diagnosis because of its clear decision and inference modules, and its ability to display the complex causal relationships between plant variables and reveal the propagation path used for fault localization in complex systems. However, in a graph-based approach, decision-making is slow because of rule

explosion. In this paper, we present an enhanced signed directed graph that utilizes qualitative trend evaluation and a granular computing algorithm to improve the decision speed and increase the resolution of the graphical method. We integrate the attribute reduction capability of granular computing with the causal/fault propagation reasoning capability of the signed directed graph and comprehensive rules in a decision table to diagnose faults in a nuclear power plant. Qualitative trend analysis is used to solve the problems of fault diagnostic threshold selection and signed directed graph node state determination. The similarity reasoning and detection ability of the granular computing algorithm ensure a compact decision table and improve the decision result. The performance of the proposed enhanced system was evaluated on selected faults of the Chinese Fuqing 2 nuclear reactor. The proposed method offers improved diagnostic speed and efficient data processing. In addition, the result shows a considerable reduction in false positives, indicating that the method provides a reliable diagnostic system to support further intervention by operators.

This work was supported by the project of State Key Laboratory of Nuclear Power Safety Monitoring Technology and Equipment (No.K-A2019.418), the Foundation of Science and Technology on Reactor System Design Technology Laboratory (HT-KFKT-14-2017003), the technical support project for Suzhou Nuclear Power Research Institute (SNPI) (No. 029-GN-B-2018-C45-P.0.99-00003), and the project of the Research Institute of Nuclear Power Operation (No. RIN180149-SCCG).

✉ Yong-Kuo Liu
LYK08@126.com

- ¹ State Key Laboratory of Nuclear Power Safety Monitoring Technology and Equipment, Shenzhen 518172, Guangdong, China
- ² Fundamental Science on Nuclear Safety and Simulation Technology Laboratory, Harbin Engineering University, Harbin 150001, China
- ³ Lianyungang JARI Deepsoft Technology Co., Ltd., Lianyungang 222002, China

Keywords Nuclear power plants · Fault diagnosis · Signed directed graph · Decision table · Granular computing

1 Introduction

As a result of the recent increase in energy demand and degradation of the natural environment by fossil fuel use, nuclear energy has attracted increasing attention as one of the most important sources of clean energy. However, the nuclear power plant (NPP) is a complex system. Its equipment and structures are complex and expensive, and

the potential for radiological hazard is always present. Leakage of radioactive material from a nuclear plant could have disastrous consequences for both humans and the environment. Human error in plant operation has been found to be a major factor in nuclear plant accident propagation. For instance, Japan's Fukushima NPP accident of 2011 was partly a result of the slow response of the operators because they could not properly predict the fault propagation path and locate the source of the fault on time [1]. Consequently, the issue of safety has a significant effect on rapid and efficient development of the nuclear power industry. In order to ensure safe and stable operation of NPPs, it is necessary to monitor the condition of NPP systems. When anomalies are discovered, fault diagnosis should be conducted as soon as possible to assist the operators in understanding the event and taking effective and timely measures to avoid serious consequences.

An effective fault diagnostic system can detect the cause of a problem quickly and accurately when exceptions occur in NPPs, giving the operator sufficient time to take the appropriate safety measures to ensure the safety of the NPP. Beyond the diagnostic speed, an effective diagnostic system should provide a clear and transparent decision visualization so as to increase the trustworthiness and reliability of the system. Many fault diagnosis methodologies have been proposed in the literature, ranging from the model-based approach [2, 3] to data-driven methods [4–6] and process-history-based methods [7]. However, precise physics models are hard to establish; further, data-driven models rely strongly on the quality of training data, and obtaining real system data that represent most fault events is difficult. Unlike conventional quantitative-based or data-driven approaches, the signed direct graph (SDG) model uses a comprehensive graphical formalism for fault diagnosis, does not require a precise mathematical description or complete operational data, and can be developed from partial information of the state equations or the operator's experience [3]. In addition, the SDG reveals the latent dangers and propagation rules in a simple and effective way, an essential requirement for fault diagnosis in NPPs. The SDG has been applied to diagnose faults in nuclear plant components [8, 9] and in a multi-energy thermo-fluid system [10]; further, the homomorphism and computational complexity problems of the SDG have been investigated [11]. An SDG model was also integrated into a fuzzy inference and multivariate system to analyze the root cause of faults in the Tennessee Eastman process [12]. However, the traditional SDG method of fault diagnosis requires a comprehensive search and inference system, especially when the search object is a complex SDG model. This makes the computation very large, resulting in poor real-time performance.

Moreover, in most complex engineering applications, a single diagnostic technique cannot effectively solve the problem of fault diagnosis. Hence, improving the fault diagnosis method by building hybrid systems has been the subject of a number of research works [5–8]. The granular computing (GrC) algorithm is a classical technique for evaluating fuzzy set problems on the basis of heuristic knowledge synthesis and attribute reduction [13]. GrC capability has been used to analyze the fuzziness of attributes in object sets and subsets [13]. It has also been used for automatic rule extraction and data processing on large datasets [14], to solve least-squares problems in quantum theory [15], and in rough set approximation [16]. Further, the attribute reduction capability has been compared with that of other algorithms [17].

Considering the complexity of the nuclear plant system, it may take a long time for conventional SDG models to calculate the relationships between many adjacent nodes and determine the fault type. In this study, we solved the time delay problem by integrating a decision table into the SDG fault diagnosis model to rapidly obtain the fault propagation path and to avoid the repeated search and inference common to conventional SDG models. In order to reduce the complexity of the decision table and further enhance the diagnostic process, the GrC algorithm was introduced. We utilized the attribute reduction capability of the GrC-based algorithm to remove redundant attributes, reduce the size and complexity of the knowledge base, and improve the efficiency of data processing. Moreover, the qualitative trend analysis (QTA) and threshold methods are used for condition monitoring. First, the GrC-SDG model uses diagnostic rule matching and similarity computing to find the fault pattern; this method takes less time than the conventional SDG method. Second, if rule matching fails, the more reliable SDG model with the threshold and QTA methods finds the fault pattern and shows the fault propagation path. Hence, the final GrC-SDG model combines the speed of the GrC algorithm and the intuitiveness of the SDG method. The integrated method results in an enhanced fault diagnosis system, which is subsequently applied for condition monitoring, fault diagnosis, and fault propagation analysis in a nuclear plant, resulting in significant improvement over the traditional SDG model.

The paper is organized as follows: Sect. 2 briefly describes the theory of the GrC-SDG method of condition monitoring. Sections 3 and 4 present the diagnostic rules and theory of GrC, respectively. Section 5 focuses on the implementation of the proposed method. In Sect. 6, we describe the experiments and results. Section 7 presents concluding remarks.

2 Theory of GrC-SDG for condition monitoring

Our SDG model relies on two basic techniques to integrate qualitative process knowledge for condition monitoring. The techniques are the threshold method and QTA. These techniques serve as the backbone of the SDG and enhance its ability to display the main connectivity in describing system faults and dependencies. A brief description of the threshold and QTA methods and their application is given below.

2.1 Threshold method

The condition monitoring system monitors the real-time data from relevant nodes of the equipment, analyzes and verifies the operating status of the equipment, and ensures the safe and reliable operation of the equipment. The state of each node in the SDG is determined by setting the upper and lower limits. When the threshold exceeds the upper limit, the node state is positive, and it is represented by + 1. When the threshold is below the lower limit, the node state is negative and is expressed as - 1, whereas when it is between the upper and lower limits, the node state is normal, and it is expressed as 0.

The implementation of this method is clear. However, considering the transient states of an operating nuclear plant, the upper and lower limit values rely on expert judgment based on sound heuristic and empirical justification. Justification is necessary because if the selected range is inaccurate, the system is prone to a high false alarm rate.

2.2 Qualitative trend analysis method

The QTA method is used to analyze the trend characteristics of the variables from a large set of data so as to determine the state and development rate of the system. QTA can be used to monitor the state and obtain the trend of variables. Trend monitoring is required to fit the data in time so as to determine the trend of the variables.

The most commonly used method of data fitting is the least-squares method [4]. Assume that n data are collected in a certain period of time and are represented by the set $(x_1, y_1), (x_2, y_2), \dots, (x_n, y_n)$, where y_n represents the value of the variable collected at time x_n . Then, the sample regression model is expressed as [4]

$$\hat{y}_i = \hat{\beta}_0 + \hat{\beta}_1 x_i, \tag{1}$$

where $\hat{\beta}_1$ is the deviation in the parameter trend, and $\hat{\beta}_0$ is the constant in the parameter trend.

Then, the sampling error is expressed as

$$e_i = y_i - \hat{y}_i = y_i - \hat{\beta}_0 - \hat{\beta}_1 x_i, \tag{2}$$

where e_i is the error in the sample (x_i, y_i) .

Further, the square loss function is given by

$$Q = \sum_{i=1}^n e_i^2 = \sum_{i=1}^n (y_i - \hat{\beta}_0 - \hat{\beta}_1 x_i)^2. \tag{3}$$

The data are better fitted when Q is calculated hourly; $\hat{\beta}_1$ reflects the trend of the variable.

Setting the partial derivative of Eq. (3) to 0 gives

$$\frac{\partial Q}{\partial \hat{\beta}_1} = 2 \sum_{i=1}^n (y_i - \hat{\beta}_0 - \hat{\beta}_1 x_i)(-x_i) = 0. \tag{4}$$

Then,

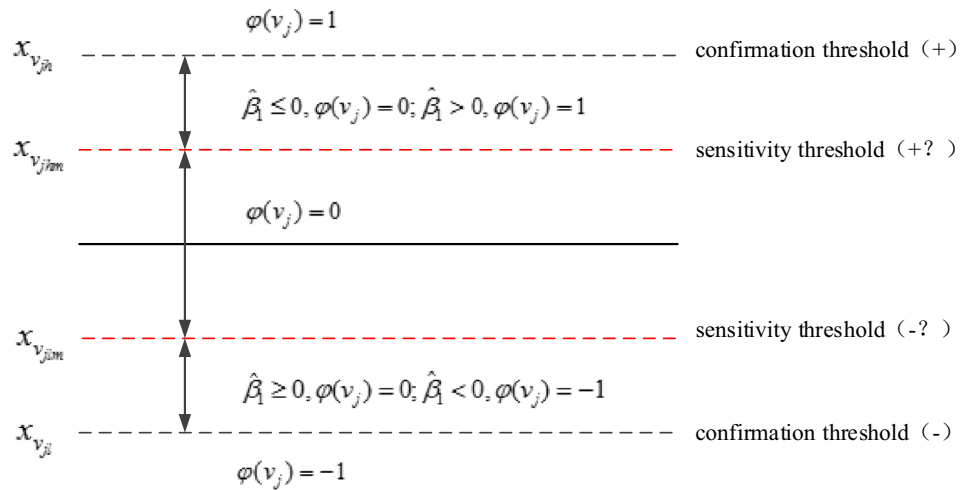
$$\hat{\beta}_1 = \frac{n \sum_{i=1}^n x_i y_i - \sum_{i=1}^n x_i \sum_{i=1}^n y_i}{n \sum_{i=1}^n x_i^2 - \sum_{i=1}^n (x_i)^2}. \tag{5}$$

When $\hat{\beta}_1$ is above the upper limit of the trend threshold, the variable has an increasing trend. By contrast, when $\hat{\beta}_1$ is below the lower limit of the trend threshold, the variation trend of the variable is considered to have decreased. If it stays within the limit, the variable is considered to be stable, and the plant is considered to be in a steady state.

We leveraged the relative strengths of the two monitoring methods, the threshold and QTA methods, to implement state monitoring of an NPP to obtain alarm signals. The actual implementation is as follows. Each component is represented by a node, and the confirmation threshold and sensitivity threshold are used to determine the current variable state of a particular node. When the value of the variable is within the sensitivity threshold, the node is in the steady state. When the value of the variable exceeds the confirmation threshold, the state of the node is determined to be abnormal at that time. If the parameter value is between the sensitivity threshold and the confirmation threshold, the node status cannot be determined. In this case, we use the QTA method to extract the trend changes for further evaluation.

When the value of the variable remains between the sensitivity threshold and the confirmation threshold for 4 s, the data generated in these 4 s are linearly fitted by the least-squares method to obtain the trend segment. Then, the fitted trend is compared with the variable trend obtainable during normal operation. If there is a match, the node is considered normal. Otherwise, the state of this node is considered to be abnormal. Figure 1 shows the sensitivity and confirmation thresholds. The mathematical expression of the node state estimation function is given as

Fig. 1 Sensitivity and confirmation thresholds



$$\psi(v_j) = \begin{cases} -1, & \text{if } x_{vj} < x_{vjl} \\ -1, & \text{if } x_{vjl} \leq x_{vj} < x_{vjm}, \hat{\beta}_1 < 0 \\ 0, & \text{if } x_{vjl} \leq x_{vj} < x_{vjm}, \hat{\beta}_1 \geq 0 \\ 0, & \text{if } x_{vjm} \leq x_{vj} < x_{vjhm} \\ 0, & \text{if } x_{vjhm} < x_{vj} \leq x_{vjh}, \hat{\beta}_1 \leq 0 \\ +1, & \text{if } x_{vjhm} < x_{vj} \leq x_{vjh}, \hat{\beta}_1 > 0 \\ +1, & \text{if } x_{vj} > x_{vjh} \end{cases} \quad (6)$$

where h is the highest value of the positive confirmation threshold, l is the lowest value of the negative confirmation threshold, and m is a mid-range value that signifies the sensitivity thresholds of the selected x_{vj} value. In this paper, we discuss single faults, where most of the variable changes are linear, although those of a small number of variables are nonlinear; hence, the nonlinear variables do not affect the positive or negative value of $\hat{\beta}_1$ calculated by the least-squares method. The threshold and QTA methods determine whether the node is abnormal using the positive or negative value of $\hat{\beta}_1$, enabling application of the QTA technique to NPP condition monitoring.

3 Integration of SDG with diagnostic rules

3.1 SDG model

SDG is a signed, directed acyclic graphical formalism applied to qualitative fault diagnosis.

Its major advantages are its graphical nature and causal reasoning ability. The main components are networked causal nodes and signed arcs linking the nodes for easy analysis. Mathematically, it is defined as follows [18]:

$$G = (V, E, \varphi, \psi), \quad (7)$$

where $V = \{v_i\}$ is the node set, which represents the variables from which the fault root cause is extracted; $E = \{e_m\}$ is the branch set, which represents the interaction between different nodes; and $\varphi(e_k)(e_k \in E)$ is the sign on branch e_k , where a positive impact is represented by a plus sign, and a negative impact is represented by a minus sign. $\psi(v_j)(v_j \in V)$ defines the sign of node v_j , which represents the status of the node: $\psi:V \rightarrow \{+, 0, -\}$.

The node state value of each conventional SDG model is determined according to the upper and lower limits of the respective variable state, as expressed in Eq. (8):

$$\psi(v_j) = \begin{cases} -1, & \text{if } x_{v_j} < x_{vjl} \\ 0, & \text{if } x_{vjl} \leq x_{v_j} < x_{vjh} \\ +1, & \text{if } x_{v_j} \geq x_{vjh} \end{cases} \quad (8)$$

where x_{v_j} represents the actual value of the variable node, and x_{vjl} and x_{vjh} are the lower and upper limits of the corresponding variable, respectively. Only two thresholds are used to determine the node state in this method. When the thresholds are too broad, this method cannot detect abnormal states in time. When the thresholds are too narrow, this method may cause a false alarm. To make sure the node state is correct, we use Eq. (6) with more thresholds to determine the SDG node state.

If the product of the contiguous node states $\psi(v_i)$ and $\psi(v_j)$ is the same as the branch symbol $\varphi(e_{ij})$ between node i and node j , that is, if the product of these three is +1, then the path $i - e_{ij} - j$ is defined as a consistent path.

3.2 SDG diagnostic rules

For every fault node added to a traditional SDG model, the computational complexity of the search tends to increase geometrically, resulting in a combinatorial explosion [7]. Consequently, we propose an SDG fault

diagnosis method that utilizes diagnostic rules. The diagnostic process involves extracting diagnostic rules from prior successful diagnosis cases, generating decision tables, and storing the tables in the diagnostic rule base. When the system is diagnosed in real time, and a residual is generated in a node, the state of the collected nodes is matched concurrently with the diagnostic rules in the decision table. If there is a successful match, the diagnosis result corresponding to the residual is displayed. Otherwise, the SDG method based on bidirectional reasoning is activated to diagnose the fault and output the result. In bidirectional reasoning, a complete search is performed with inverse correlation with the abnormal node, and all possible fault sources that induced the abnormality are obtained. Then, starting from these fault sources, forward reasoning is performed in turn, and incorrect fault sources are removed. Finally, the correct fault and propagation paths are obtained [8]. Subsequently, the new diagnostic rules are extracted and added to the previous decision table to form a new decision table and update the diagnostic rule base.

4 Granular computing

4.1 Basic concepts

In current research on intelligent systems, the GrC method is used to simulate human thinking and solve complex problems [19]. Its key concept is the distillation of complex problems into a number of simple granular problems according to expert knowledge or experience and solving each of them independently. Then, the correlation between each pair of granulated, solved problems is determined to analyze and solve the larger problem. This method improves the solution of complex problems. The main theories used to analyze and solve problems at different granularities are rough set theory, word calculation theory, and quotient space theory [3, 19]. Of the three theoretical models, empirical evaluation has shown the superiority of rough set theory [19], which is selected in our work.

Rough set theory is a tool for dealing with the lower and upper approximations of imprecise information or indefinite knowledge. Assuming the decision-making condition is not changed, an attribute reduction algorithm is used to eliminate redundant attributes or features, and the simplest decision rules of the problem are obtained. Mathematically, the decision table S is defined as follows [19]:

$$S = (U, A, V, f), \tag{9}$$

where U is the decision domain, which is expressed as $U = \{x_1, \dots, x_k, \dots, x_l\}$; A is the decision attribute set, which is expressed as $A = C \cup D$; C is the condition attribute set;

and D is the decision attribute set. V represents the set of attribute values, and f represents an information function that can give the attribute value of each object in the decision domain. For an arbitrary attribute subset $P \in A$, the decision domain U divided by the knowledge P is expressed as

$$U/IND(P) = \{X_1, X_2, X_3, \dots, X_n\}, \tag{10}$$

where X_n is a granular with knowledge P , and n is the cardinality of $U/IND(P)$. If an indistinguishable relationship can be determined by P , then P can be expressed as $IND(P)$.

A bit vector of length l is used to represent X_n , where l is the cardinality of U . The i th bit of the vector is 1 if $x_i \in X_n$; otherwise, it is 0. For example, $U/a = \{\{x_1, x_4\}, \{x_2, x_3\}\}$ can be expressed as $U/a = \{1001, 0110\}$, where l equals 4.

The formula for the knowledge granularity $GD(P)$ is

$$GD(P) = \sum_{i=1}^n \frac{|X_i|^2}{|U|^2} = \frac{1}{l^2} \sum_{i=1}^n \left(\sum_{k=1}^l a_{ik} \right)^2, \tag{11}$$

where a_{ik} represents the k th bit in bit vector X_i , and $GD(P)$ represents the distinguishing ability of the knowledge P on decision domain U .

The relative granularity of knowledge Q about knowledge P can be defined as follows:

$$GD(P|Q) = GD(Q) - GD(P \cup Q), \tag{12}$$

where $GD(P|Q)$ represents the distinguishing ability of knowledge P relative to knowledge Q on decision domain U .

The importance of attribute a of R relative to D is

$$\text{sig}(a, R, D) = GD(D|R) - GD(D|R \cup a), \tag{13}$$

where a belongs to the condition attribute set C .

In essence, Eq. (13) calculates the difference between the relative granularity before and after attribute a is added to R . For greater values of $\text{sig}(a, R, D)$, attribute a is more important.

4.2 Knowledge reduction

A common deficiency of a decision table is that some of the node information in the table is redundant. Hence, attribute reduction is necessary to further improve the diagnostic speed and reduce the computational space. The goal of attribute reduction is to ensure that the sensitivity of the attribute set to the universe is unchanged after reduction, and every element in the attribute set is also necessary [20]. Implementing an attribute reduction algorithm based on GrC would improve the quality of a decision by removing redundant attributes, resulting in a compact

decision table, a smaller and less complex knowledge base, and more efficient data processing. We integrate the attribute reduction capability of the GrC algorithm with a rule-based SDG model. The integration results in significant improvement in the diagnostic speed and saves computing resources.

The specific steps involved in utilizing the relative granularity attribute reduction algorithm to reduce the decision table are as follows:

- (1) Merge the same rules in the decision table and set the reduction result $RED = \varphi$;
- (2) Calculate $sig(c_i, RED, D) = GD(D|RED) - GD(D|RED \cup c_i)$, $c_i \in C \setminus RED$;
- (3) Select the attribute c_i corresponding to the maximum value as c_k . If there are multiple attributes that satisfy the condition, select the first attribute as c_k ;
- (4) If $sig(c_k, RED, D) > 0$, and $RED = RED \cup c_k$, go to step (2) to continue the cycle calculation. Otherwise, end the cycle and output RED.

The attribute reduction process of the algorithm is shown in Fig. 2, and a flowchart of the diagnosis process is shown in Fig. 3. As Fig. 3 shows, this study uses the

Fig. 2 Flowchart of the reduction algorithm

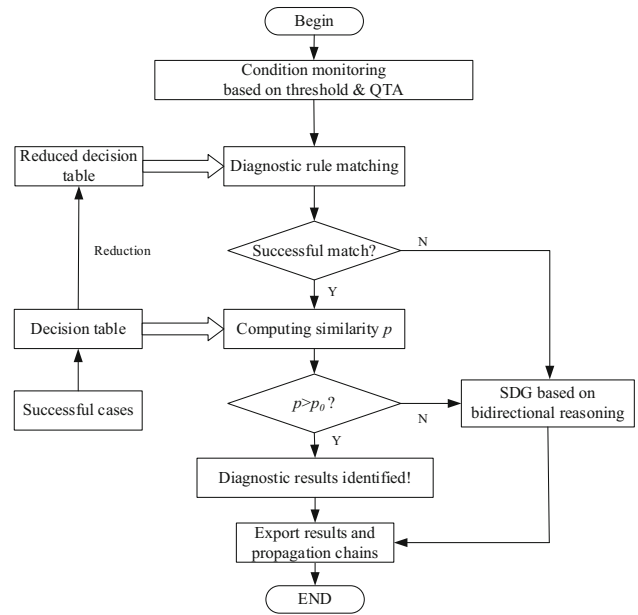
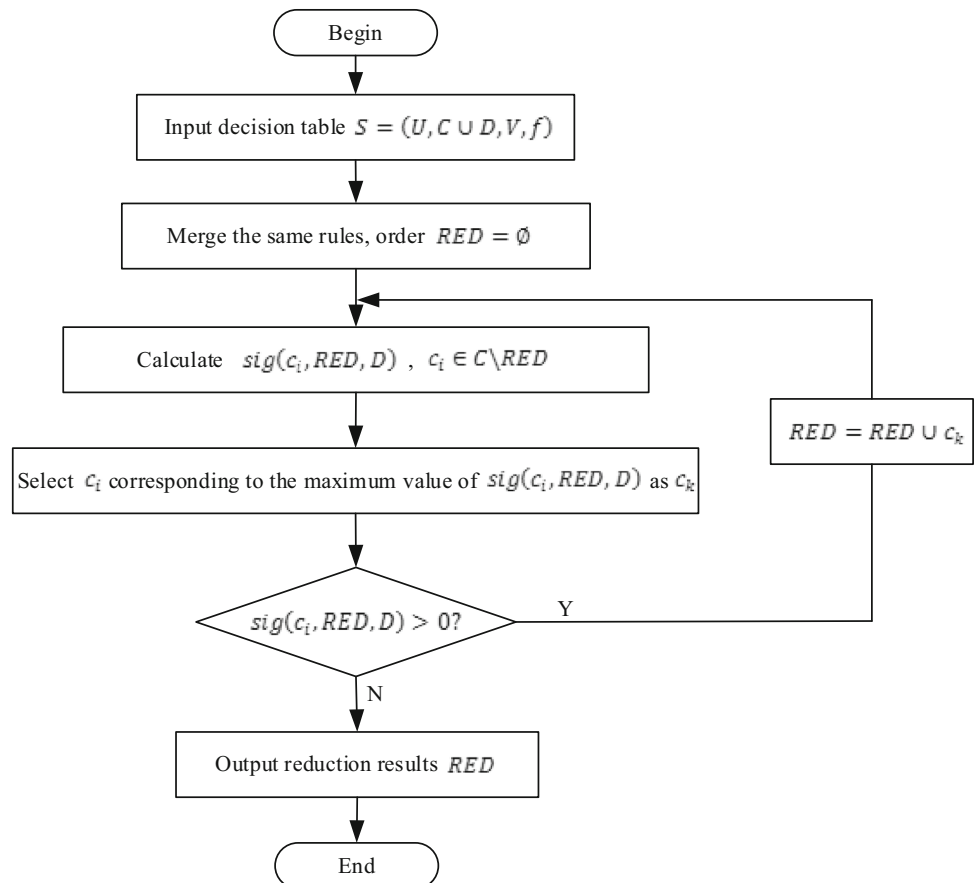


Fig. 3 Flowchart of SDG based on GrC-SDG

similarity determined by the GrC-based algorithm to ensure the correctness of the decision results. The similarity p between the decision granular $G = (\varphi, m(\varphi))$ and

the condition granular $G' = (\varphi', m(\varphi'))$ can be expressed as

$$p = \text{card}(G' \otimes G) / \text{card}(G) \quad (G \neq \Phi), \tag{14}$$

where card represents the number of element in granular G or G' , and \otimes represents the *and* operation between two binary granular structures.

To calculate the binary granular of each attribute, we need the time complexity of $O(|U|)$. Under the worst condition, the entire GrC attribute reduction method requires a time complexity of $|U| \times |C| + |U| \times (|C| - 1) + \dots + |U| = (|C| + 1) \times |C| \times |U| / 2$. Thus, the total time complexity of the method is $O(|C|^2|U|)$. Moreover, it is much faster than the heuristic attribute reduction algorithm given in the literature, an instance of which is found in [20] with a time complexity of $O(|C|^2|U|^2)$.

4.3 Fault diagnosis system

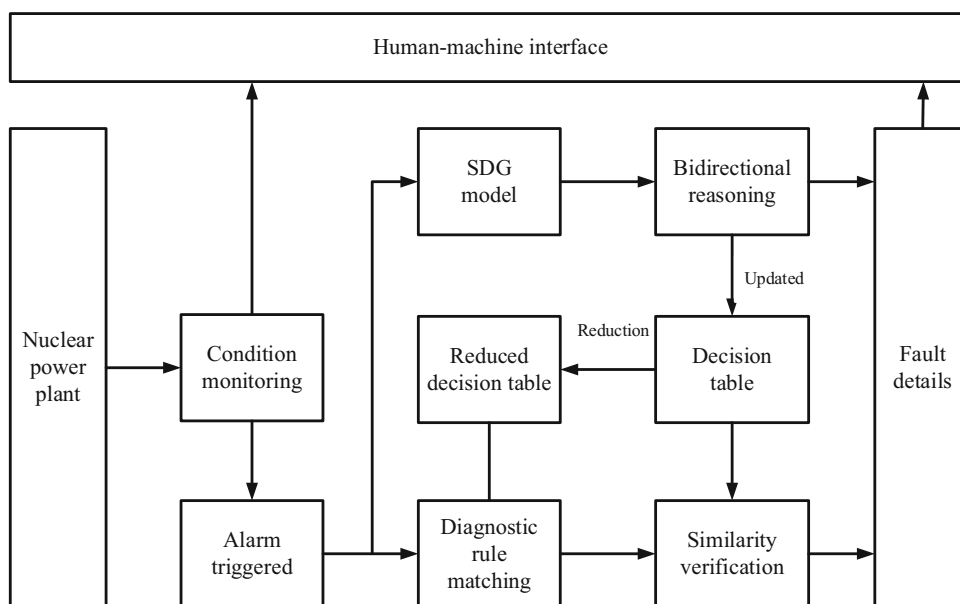
The process design of this system is shown in Fig. 4. The operating variables of the NPP are monitored in real time. The values of the important operating variables are displayed in the human-machine interface, and condition monitoring is carried out by the threshold and QTA methods. When an alarm signal appears, the instantaneous signal is immediately matched with the reduced decision table and verified by similarity reasoning. If there is a successful match, the fault type and fault propagation path are output. Otherwise, the SDG model is activated for bidirectional reasoning; then, the fault type and fault propagation path are obtained.

5 Demonstration of GrC-SDG model for NPP fault diagnosis

5.1 Establishment of SDG model

To demonstrate the implementation of the proposed GrC-SDG model in a form suitable for diagnosing actual faults in a real plant, we considered the Fuqing NPP, Unit 2, and selected seven typical faults for case study and analysis. These faults are small break loss-of-coolant accident (LOCA), steam generator tube rupture (SGTR), main steam line break (MSLB), inadvertent withdrawal of control rod (Withdrawal), inadvertent insertion of control rod (Insertion), and loss-of-feed water (LOFW). For the MSLB event, two scenarios are considered: an in-containment break and another break outside the containment. We simulated this fault using the Personal Computer Transient Analyzer (PCTTRAN) software. PCTTRAN is used to simulate a variety of accident and transient conditions for NPPs; it displays the status of important variables and allows simulation of operator actions by interactive control [21]. Here, the initial conditions in PCTTRAN are selected using operation data from the Fuqing 2 NPP to simulate the operating condition of Fuqing 2 NPP. The Fuqing 2 NPP is one of the CPR-1000 pressurized water reactors (PWRs) selected for the first four units of the Fuqing nuclear plant. The Chinese-developed CPR-1000 is an improvement on the Areva-designed PWRs at the Daya Bay Nuclear Power Plant. This CPR-1000 has design net capacities of 1000 MWe and 2905 MWt and has been commercially operated by China’s CNNC Fujian Fuqing Nuclear Power Co., Ltd., since 2015.

Fig. 4 Flowchart of the fault diagnosis system for NPP



The GrC algorithm with the SDG model is integrated with C# programming language to form a usable human-machine interface (as shown in Fig. 7), and the data from the fault simulations on PCTTRAN are utilized as inputs for the hybrid model. Quantitative analysis is performed according to the selected fault types, and 32 relevant variables are selected, as shown in Table 1. The SDG model of the NPP is presented in Fig. 5; the solid lines indicate a positive impact between adjacent nodes, where the nodes change in the same direction. The dashed lines represent negative impacts, where adjacent nodes change in opposite directions.

Table 1 Variable nodes of the SDG model of NPP

ID	Node label	Node name	Units
1	PL1	Pressure of loop 1	Pa
2	PL2	Pressure of loop 2	Pa
3	PL3	Pressure of loop 3	Pa
4	CFL1	Coolant flow of loop 1	kg/s
5	CFL2	Coolant flow of loop 2	kg/s
6	CFL3	Coolant flow of loop 3	kg/s
7	TCL1	Temperature of cold leg 1	°C
8	TCL2	Temperature of cold leg 2	°C
9	TCL3	Temperature of cold leg 3	°C
10	THL1	Temperature of hot leg 1	°C
11	THL2	Temperature of hot leg 2	°C
12	THL3	Temperature of hot leg 3	°C
13	SPSGA	Steam pressure of SG A	Pa
14	SPSGB	Steam pressure of SG B	Pa
15	SPSGC	Steam pressure of SG C	Pa
16	WLSGA	Water level of SG A	m
17	WLSGB	Water level of SG B	m
18	WLSGC	Water level of SG C	m
19	FFSGA	Feedwater flow of SG A	kg/s
20	FFSGB	Feedwater flow of SG B	kg/s
21	FFSGC	Feedwater flow of SG C	kg/s
22	SFSGA	Steam flow of SG A	kg/s
23	SFSGB	Steam flow of SG B	kg/s
24	SFSGC	Steam flow of SG C	kg/s
25	PP	Pressurizer pressure	Pa
26	PWL	Pressurizer water level	m
27	PRB	Pressure of reactor building	MPa
28	TRB	Temperature of reactor building	°C
29	RRB	Radioactivity of reactor building	C/kg
30	WLRB	Water level of reactor building	m
31	NP	Nuclear power	KW
32	EP	Electric power	MW

5.2 Decision table reduction

To improve the computation and diagnostic efficiency, we establish the diagnostic rules and generate decision tables according to prior fault cases in the Fuqing 2 NPP, in combination with the SDG model. When the same type of fault occurs again, the diagnostic results can be obtained according to the matching degree of the diagnostic rules.

Using the instances of successful fault diagnosis, the 32 node variables related to the SDG model are taken as the condition attributes to generate the decision table for the NPP fault diagnosis. This decision table results in a large number of diagnostic rules. Table 2 displays a section of the decision table.

In Table 2, there are a large number of redundant attributes in the decision table, and the number of diagnostic rules varies. The attribute explosion affects the rule matching and diagnostic speed. Hence, we reduce the attributes while retaining the fault diagnosis reliability using the attribute reduction capability of the GrC algorithm. The relative granularity attribute reduction algorithm is used for the calculation in the program, and the final reduced results are shown in Table 3.

Table 3 shows that the number of node variables required by rule matching has been reduced from 32 to 4, and the number of rules has been reduced from 80 to 14, which significantly simplifies the decision tables and improves the matching speed of the diagnostic rules.

Figure 6 shows the decision table update interface. As described in Sect. 3.2, when rule matching fails, SDG bidirectional reasoning is activated. After diagnosis, the new diagnostic rules are recorded in the manual, and decision table reduction is executed again to update the diagnostic rules.

6 Results and discussion

6.1 Steam generator tube rupture (SGTR)

For the simulated rupture in a Fuqing 2 steam generator tube, a heat transfer tube was simulated in steady-state full-power operation. We inserted the rupture and observed the rate of deviations of the variables. At 1 s after fault insertion, deviations were observed in 8 variables. In the following 3 s, the number of deviating variables increased to 17. The propagation path of the fault was refined, and the display of the condition monitoring and diagnosis system is shown in Fig. 7. The variables in the human-machine interface are shown in Table 1. Rule matching is performed according to Table 3. As shown in Fig. 8, the attribute values of WLSGC, PRB, CFL1, and SFSGA in this test result are 0, 0, -1, and 1, which match the seventh rule of

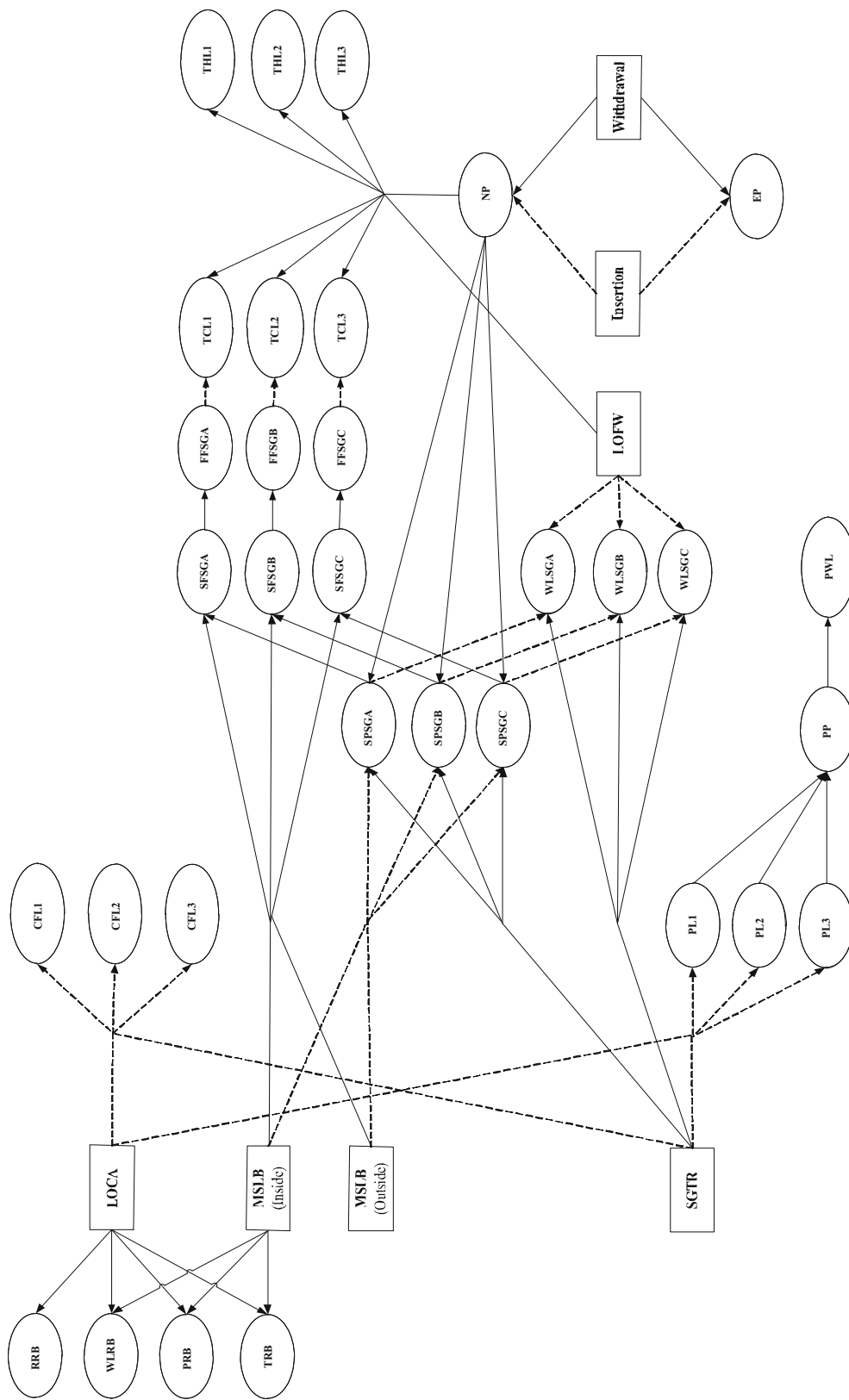


Fig. 5 SDG model of NPP



Fig. 7 Results of state monitoring and fault diagnosis of SGTR

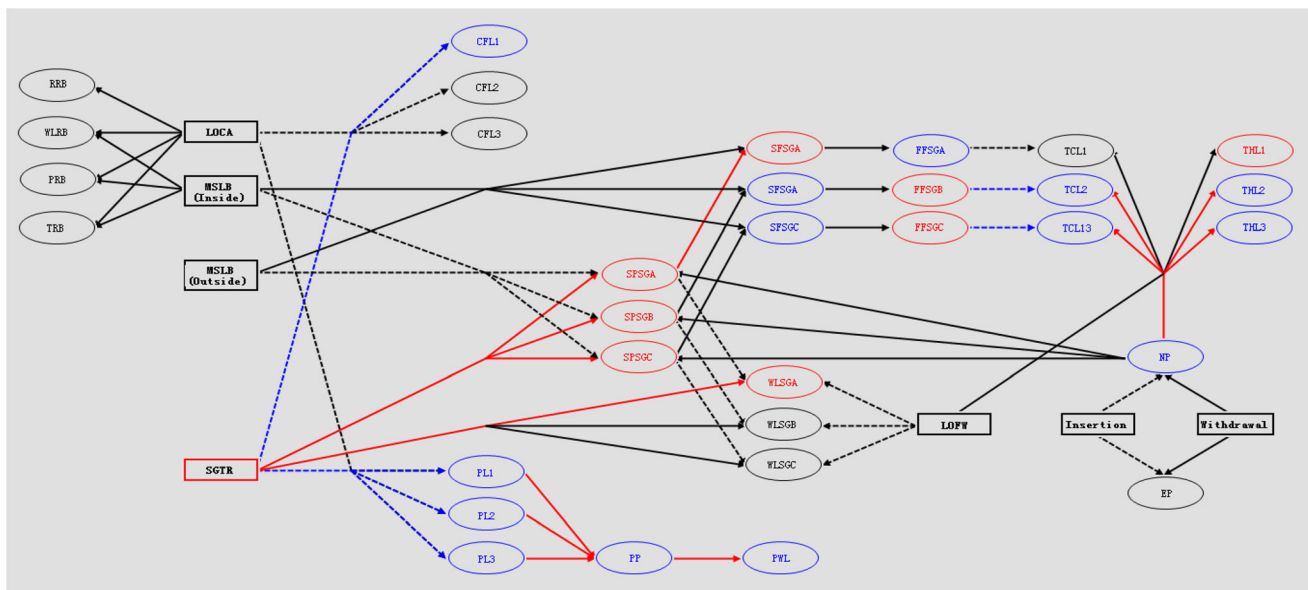


Fig. 8 Result of SDG path reasoning for SGTR

with the expert’s heuristic diagnosis of the simulated fault. When the control rod is accidentally inserted, negative reactivity is introduced, resulting in a reduction in nuclear power. The temperatures of the cold legs and hot legs decrease, the heat transfer capacity of the SG decreases, and the steam pressure of the SG drops, which results in a decrease in the steam flow in the SG.

Figure 10 shows the fault propagation path for insertion and the forward reasoning of the SDG model. The fault propagation and analysis are as follows:

- Insertion → Nuclear power → Steam pressure of SG A → Steam flow of SG A
- Insertion → Nuclear power → Steam pressure of SG B → Steam flow of SG B
- Insertion → Nuclear power → Steam pressure of SG C → Steam flow of SG C
- Insertion → Nuclear power → Temperature of cold leg 1
- Insertion → Nuclear power → Temperature of cold leg 2
- Insertion → Nuclear power → Temperature of cold leg 3
- Insertion → Nuclear power → Temperature of hot leg 1



Fig. 9 Result of state monitoring and fault diagnosis for control rod insertion

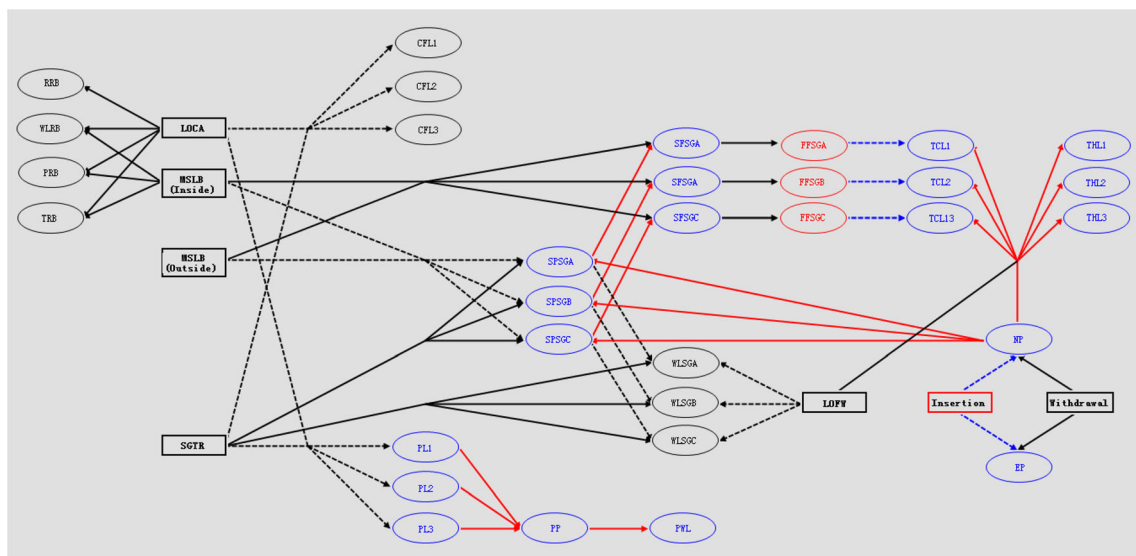


Fig. 10 Result of SDG path reasoning for insertion

Insertion → Nuclear power → Temperature of hot leg 2
 Insertion → Nuclear power → Temperature of hot leg 3
 Insertion → Electric power

7 Conclusion

In this study, we presented a rule-based GrC-SDG method for nuclear plant fault diagnosis. Plant condition monitoring is performed using a combination of the threshold method and QTA. Fault is detected when a measured variable deviates from a predetermined

threshold. The fault is localized and isolated using the causal graph output from the SDG and the decision table. To simplify the decision table rules and eliminate redundant variables, the attribute reduction capability of GrC is introduced. The resulting decision table is then integrated into the SDG fault diagnosis method to improve the diagnostic process and improve the diagnostic speed. The main contribution in this study is summarized as follows:

1. We developed a multifunctional rule-based GrC-SDG fault diagnosis system using the QTA and threshold methods and performed functional tests on sample faults from a simulation of the Chinese Fuqing 2 nuclear reactor.
2. The QTA and threshold condition monitoring algorithm, GrC algorithm, and SDG model were integrated into a human-machine interface using the C# programming language.
3. The diagnostic system was evaluated using the data obtained from simulated faults. The results showed that the rule-based GrC-SDG method diagnosed the faults accurately, and the SDG produced a clear and concise causal graph devoid of redundant paths.
4. The GrC-SDG method was shown to be intuitive, highly sensitive, and suitable for condition monitoring and early fault diagnosis. In addition, the visual and spatial representation of the diagnostic result enables faster fault recognition and decision-making by the operators.

We observed that for incipient faults where the rate of change of certain variables is small, the monitoring system displays a steady state. In addition, common plant transients such as a sudden spike in the measured values of variables are also not detectable if the spike is brief, and a false negative is generated. A modality to address these limitations will be the focus of our future research.

References

1. Y. Fujita, Learning from the Fukushima nuclear power plant accident—a resilience point of view, in *2012 Southeast Asian Network of Ergonomics Societies Conference (SEANES)* (2012), pp. 1–5. <http://dx.doi.org/10.1109/SEANES.2012.6299591>
2. V. Venkat, R. Raghunathan, Y. Kewen et al., A review of process fault detection and diagnosis part I: quantitative model-based methods. *Comput. Chem. Eng.* **27**(3), 313–326 (2003). [https://doi.org/10.1016/S0098-1354\(02\)00160-6](https://doi.org/10.1016/S0098-1354(02)00160-6)
3. G. Xie, X. Wang, K. Xie, SDG-based fault diagnosis and application based on reasoning method of granular computing, in *IEEE Conf. Cont. Dec.* (2010), pp. 1718–1722. <http://dx.doi.org/10.1109/CCDC.2010.5498443>
4. A. Ayodeji, Y.K. Liu, H. Xia, Knowledge-base operator support system for nuclear power plant fault diagnosis. *Prog. Nucl. Energy* **105**, 42–50 (2018). <https://doi.org/10.1016/j.pnucene.2017.12.013>
5. Y.K. Liu, A. Ayodeji, Z.-B. Wen et al., A cascade intelligent fault diagnostic technique for nuclear power plants. *J. Nuclear Sci. Technol.* **55**(3), 1–13 (2018). <https://doi.org/10.1080/00223131.2017.1394228>
6. A. Ayodeji, Y.K. Liu, SVR optimization with soft computing algorithms for incipient SGTR diagnosis. *Ann. Nuclear Energy* **121**, 89–100 (2018). <https://doi.org/10.1016/j.anucene.2018.07.011>
7. M.A. Kramer, B.L. Palowitch Jr., A rule-based approach to fault diagnosis using the signed directed graph. *Am. Inst. Chem. Eng. J.* **33**(7), 1067–1078 (1987). <https://doi.org/10.1002/aic.690330703>
8. Z. Zhang, C. Wu, B. Zhang et al., SDG multiple fault diagnosis by real-time inverse inference. *Rel. Eng. Syst. Saf.* **87**(2), 173–189 (2005). <https://doi.org/10.1016/j.res.2004.04.008>
9. G.H. Wu, Y.K. Liu, C.L. Xie, Research on fault diagnosis based on SDG-QTA in nuclear power plants. *Atom. Energy Sci. Technol.* **50**(8), 1467–1473 (2016). <https://doi.org/10.7538/yz.2016.50.08.1467>. (in Chinese)
10. R. Smaili, R.E. Harabi, M.N. Abdelkrim, Design of fault monitoring framework for multi-energy systems using signed directed graph. *IFAC PapersOnline* **50**(1), 15734–15739 (2017). <https://doi.org/10.1016/j.ifacol.2017.08.2304>
11. R.C. Brewster, F.F. Foucaud et al., The complexity of signed graph and edge-coloured graph homomorphisms. *Discrete Math.* **340**(2), 223–235 (2017). <https://doi.org/10.1016/j.disc.2016.08.005>
12. B. He, T. Chen, X. Yang, Root cause analysis in multivariate statistical process monitoring: Integrating reconstruction-based multivariate contribution analysis with fuzzy-signed directed graphs. *Comput. Chem. Eng.* **64**, 167–177 (2014). <https://doi.org/10.1016/j.compchemeng.2014.02.014>
13. G. Chiaselotti, T. Gentile, F. Infusino, Granular computing on information tables: families of subsets and operators. *Inf. Sci.* **442**, 72–102 (2018). <https://doi.org/10.1016/j.ins.2018.02.046>
14. S. Butenkova, A. Zhukova, A. Nagoro et al., Granular computing models and methods based on the spatial granulation. *Proc. Comput. Sci.* **103**, 295–302 (2017). <https://doi.org/10.1016/j.procs.2017.01.111>
15. M. Wang, M. Wei, Y. Feng, An iterative algorithm for least squares problem in quaternionic quantum theory. *Comput. Phys. Commun.* **179**(4), 203–207 (2008). <https://doi.org/10.1016/j.cpc.2008.02.016>
16. Y.Y. Yao, Information granulation and rough set approximation. *Int. J. Intell. Syst.* **16**(1), 87–104 (2001). [https://doi.org/10.1002/1098-111X\(200101\)16:1%3C87:AID-INT7%3E3.0.CO;2-S](https://doi.org/10.1002/1098-111X(200101)16:1%3C87:AID-INT7%3E3.0.CO;2-S)
17. Y. Yao, Y. Zhao, Attribute reduction in decision-theoretic rough set models. *Inf. Sci.* **178**(17), 3356–3373 (2008). <https://doi.org/10.1016/j.ins.2008.05.010>
18. Y.K. Liu, G.H. Wu, C.L. Xie, A fault diagnosis method based on signed directed graph and matrix for nuclear power plants. *Nucl. Eng. Des.* **297**, 166–174 (2016). <https://doi.org/10.1016/j.nucengdes.2015.11.016>
19. T.Y. Lin, Granular computing on binary relations II: rough set representations and belief functions. *Rough Sets Knowl. Discov.* **1**, 121–140 (1998)
20. X. Hu, N. Cercone, Learning in relational databases: a rough set approach. *Comput. Intell.* **11**(2), 323–337 (1995). <https://doi.org/10.1111/j.1467-8640.1995.tb00035.x>
21. Y.H. Cheng, C. Shih, S.C. Chiang et al., Introducing PCTRAN as an evaluation tool for nuclear power plant emergency responses. *Ann. Nuclear Energy* **40**(1), 122–129 (2012). <https://doi.org/10.1016/j.anucene.2011.10.016>